RSC Advances

ROYAL SOCIETY OF CHEMISTRY

www.rsc.org/advances

One-pot electrochemical synthesis of polydopamine coated magnetite nanoparticles

Eva Mazario,[a] *Jorge Sánchez-Marcos,*[a] *Nieves Menéndez,*[a] *Pilar Herrasti,*[a] *Mar García-Hernández,*[b] *Alexandra Muñoz-Bonilla*[a] *

[a] Departamento de Química Física Aplicada, Facultad de Ciencias, Universidad Autónoma de Madrid, C/Francisco Tomás y Valiente, 7, Cantoblanco, 28049 Madrid, Spain.

[b] Instituto de Ciencia de Materiales de Madrid, Consejo Superior de Investigaciones Científicas, Cantoblanco, 28049 Madrid, Spain

Abstract

Herein a facile and versatile one step synthesis of magnetite nanoparticles coated with polydopamine is described. Magnetite nanoparticles are synthesized electrochemically by electrooxidation of iron in aqueous medium in the presence of dopamine. The oxidative conditions and alkaline pH involved in the synthesis favor the self-polymerization of dopamine that adheres at the surface of the magnetic nanoparticles in a simultaneous process. It is showed that the size of the magnetite nanoparticles as well as the polydopamine coating can be controlled by varying the synthetic approach that is, adding dopamine at the beginning of the electrosynthesis, in the meantime or at the end of the process. The particle size of the core varies between few nanometers and 25 nm while the shell can reach thickness up to ~5 nm. The obtained hybrid nanoparticles were characterized by thermogravimetric analysis (TGA), infrared spectroscopy (FTIR), X-ray diffraction (XRD) and transmission electron microscopy (TEM). In addition, the magnetic measurements of the different obtained materials were carried out showing a variety of magnetic behaviors depending on the synthetic procedure.

Keyword: Polydopamine; magnetic nanoparticles; electrochemical synthesis; polymer coating; superparamagnetic

Introduction

Iron oxide magnetic nanoparticles have found widespread applications in many fields covering catalysis,[1] data storage media,[2] environmental remediation separation,[3] purification[4] and biomedical uses such as magnetic resonance imaging (MRI),[5] hyperthermia[6] or drug delivery.[7] In biomedicine, superparamagnetic nanoparticles are of particular interest because in the absence of magnetic field they do not exhibit remanence magnetization and coercivity field, preventing the particle aggregation. Ferromagnetic materials, for instance magnetite or maghemite which are also chemically stable and biocompatible, could became superparamagnetic when they behave as single magnetic domains typically with sizes smaller than about 15 nm. However, large particles are more easily manipulated by external magnetic fields due to the higher magnetization saturation and are desirable in other applications. Thus, it is crucial the precise control of the size that affects the magnetic properties as well as the shape, size distribution and the surface chemistry of the nanoparticles. The surface functionality has an influence not only on the magnetic behavior of the nanoparticles but also governs the interactions with the environment including the stability and dispersability of the nanoparticles, biocompatibility, the participation in biological recognitions events, cellular up-take processes, etc.[8] In this concern polydopamine (PDA) has attracted a substantial interest to surface functionalize magnetic nanoparticles as well as other types of materials because of its unique properties.[9101112] Dopamine which was inspired from the adhesive proteins of mussels can self-polymerize in alkaline aqueous media generating polymer films that adhere onto practically all material surfaces including metals, metal oxides, polymers and ceramics.[13] It is also reported the oxidant induced polymerization of dopamine in neutral or acidic pH.[14] Besides its great adhesion ability and biocompatibility, PDA

coatings exhibit other attractive properties.[15] For example, PDA has been demonstrated to be an effective carbon source for the formation of carbon spheres, capsules and carbon-coated materials.[16,17] In addition, PDA can act as a platform to immobilize at the surface further compounds such as biomolecules or drugs through its many functional groups that are able to react with a variety of molecules including thiol and amine via Michael-type additions or Schiff base reactions.[18] The polydopamine can also bind various multivalent metal ions such as Fe^{3+}, Zn^{2+}, Cu^{2+}, etc.[19] and behaves as reducing agents conducting to the synthesis of metal NPs directly from their salts.[20] Therefore, the preparation of magnetic nanoparticles covered with PDA and with precise control of the size is received a great attention nowadays because enables versatile platforms for a wide range of applications.[21] Typically core-shell magnetic polydopamine nanoparticles are synthesized in two steps, that is, the preparation of the magnetic NPs and subsequently the formation of the PDA shell.[222324] In the current work we describe a facile one-pot synthesis of magnetite nanoparticles coated with PDA (Fe_3O_4@PDA) via electrochemical method (see Figure 1). Basically, this strategy consists in the electrochemical synthesis of magnetite nanoparticles by the oxidation of iron foils immersed in aqueous solution and the simultaneous self-polymerization of dopamine in the medium. The polydopamine formed around the nanoparticles acts as stabilizer avoiding the agglomeration of the resulting nanoparticles. Slight modifications of this main approach by varying addition order and amount of dopamine added as well as the reaction time allow the preparation of a range of nanomaterials, where the size of both the magnetic core and shell can be easily controlled, obtaining a variety of magnetic behaviors.

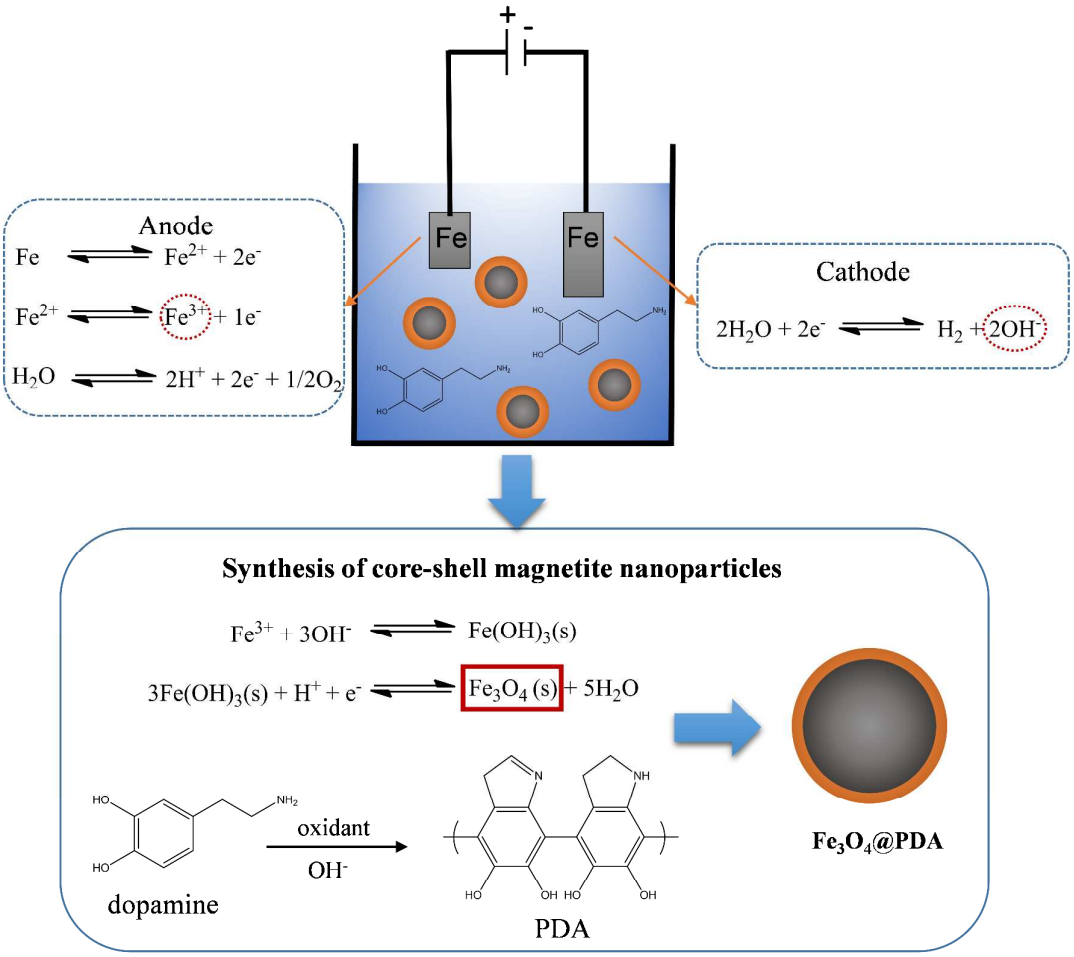

Figure 1. Schematic representation of the one-step synthesis of magnetite nanoparticles coated with polydopamine via electrochemical route.

Experimental Section

Synthesis of magnetite nanoparticles coated with polydopamine.

Magnetite nanoparticles were synthetized via electrochemical method at room temperature following a method previously developed by our group but introducing several modifications.[25] Foils of iron (99.5%, Goodfellow) were used as anode and cathode and placed perpendicular to each other. The foils were immersed in 100 mL of a NaCl (Panreac) (26 mM) aqueous solution and subsequently the current (50 m Acm^{-2})

was applied with AMEL model 549 potentiostat/galvanostat during 30 min under magnetic stirring. Based on this electrosynthesis route, three different procedures were explored in order to functionalize the surface of the magnetic NPs with polydopamine (Scheme 1), incorporating a certain amount (from 2 to 60 mg) of dopamine (99%, Aldrich) to the reaction medium.

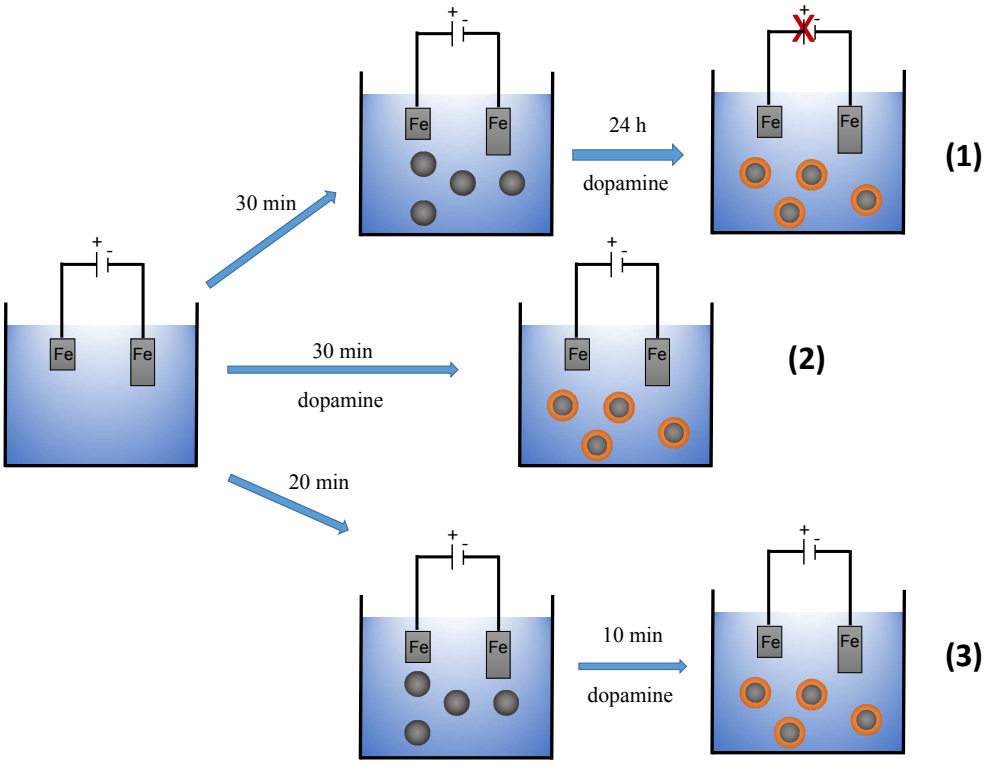

Scheme 1. Illustration of the approaches used for the electrochemical synthesis of Fe_3O_4@PDA nanoparticles.

Subsequently the obtained particles in each approach were magnetically separated from the solution and washed repeatedly with deionized water. Part of the colloid was dried under vacuum.

Measurements

The crystalline phase and the size of the crystals of the resulting magnetic nanoparticles were analyzed by X-ray diffraction in a D5000 diffractometer equipped with a

secondary monochromator and a SOL-X Bruker detector with Cu-Kα radiation. The patterns were collected from 5º to 80º 2θ with 4º min^{-1} scan rate. The diffractograms were analyzed using the Fullprof suite[26] based on the Rietveld method. Transmission electron microscope (TEM) studies were conducted with a JEOL JEM 1010 operating at acceleration voltage of 100 kV and a FEG-TEM JEOL JEM 3000 F operating at 300 kV. Uv-vis spectra were recorded on a Perkin-Elmer Lambda 35 spectrophotometer whereas the FTIR measurements were carried out on a Bruker IFS66v. The thermogravimetric analysis (TGA) of the coated nanoparticles were conducted with a TA instruments Q500 with 10 ºC min^{-1} heating rate from room temperature up to 900 ºC under air flow. The colloidal properties of the synthesized particles in terms the zeta potential were studied on a Zetasizer NanoTM, from Malvern Instruments at 25 ºC using 10^{-2} M KNO_3 as background electrolyte. Preliminary magnetic studies were carried out using a SQUID magnetometer (Quantum Design MPMS XL-5). The magnetic hysteresis loops of all samples were obtained at 100 K under a maximum applied field of 50 kOe. The magnetization versus temperature curves, M(T), were carried out in zero-field-cooling (ZFC) and field-cooling (FC) procedures under an applied field of 100 Oe.

Results and discussion

In a previous strategy,[25] magnetite nanoparticles is typically obtained by Fe electrooxidation in the presence of a surfactant such as tetramethylammonium chloride, acting as supporting electrolyte and as coating agent at the same time. As displayed in Figure 1, the mechanism of formation implies the anode oxidation to ferrous ions and ferric ions, and also the electrolysis of water. At the cathode, reduction of water takes place leading OH^- and consequently increasing the pH up to basic values. These OH^- diffuse to the anode allowing the formation of $Fe(OH)_3$ to later be reduced to Fe_3O_4. In

those synthetic conditions the surfactant normally added to the mixture, stabilizes the obtained magnetite nanoparticles. In the present work, the magnetite nanoparticles were synthesized following this method but using NaCl as electrolyte and dopamine as coating agent. Since the electrochemical synthesis of magnetic NPs involves alkaline pH and oxidative conditions it is expected the formation of polydopamine coating at the surface of the magnetite nanoparticles under those conditions. This is because the dopamine can self-polymerize at alkaline pH values[13] and also in oxidative conditions at neutral or acidic pH,[14] consequently three different strategies were explored in order to obtain a polydopamine shell.

One strategy (approach **1**, Scheme 1) consists in the formation of the core-shell nanoparticles by two consecutive steps, first the formation of magnetic nanoparticles and subsequently the addition of dopamine (0.2 mg/mL) to the reaction mixture once the current was turned off, fact that also decreases the pH of the mixture until pH 7. Therefore, the polymerization of the dopamine can be only induced by oxidative compounds present in the mixture such as Fe^{3+}.

Recently, it has been investigated the role played by the transition-metal ions, in particular Ni^{2+}, in the polymerization of dopamine in aqueous solution at pH 8.5. Ni^{2+} ions seem to mediate the polymerization reaction by complexation with dopamine oligomers that provokes an acceleration of the polymerization.[27] In this case an early polymerization step induced by basic pH is needed because dopamine is not a strong ligand for Ni^{2+} in water. Herein, Fe^{3+} as transition-metal ions exhibit a positive reduction potential in contrast to Ni^{2+} and also form complexes with dopamine through coordination bonds. Therefore, it is expected that Fe^{3+} would mediate the polymerization from the beginning of the reaction.

The PDA coating of the nanoparticles was studied analyzing the influence of the running time when the dopamine was incorporated to the mixture. Immediately after the addition of the dopamine, the dark mixture turns to dark purple color as a consequence of the oxidation of dopamine, and then a gradual change to dark was observed. After a desired time, the nanoparticles and the supernatant were both analyzed separately. The oxidant induced polymerization of dopamine was monitored by the UV-vis spectra of the supernatants as depicted in Figure 2.

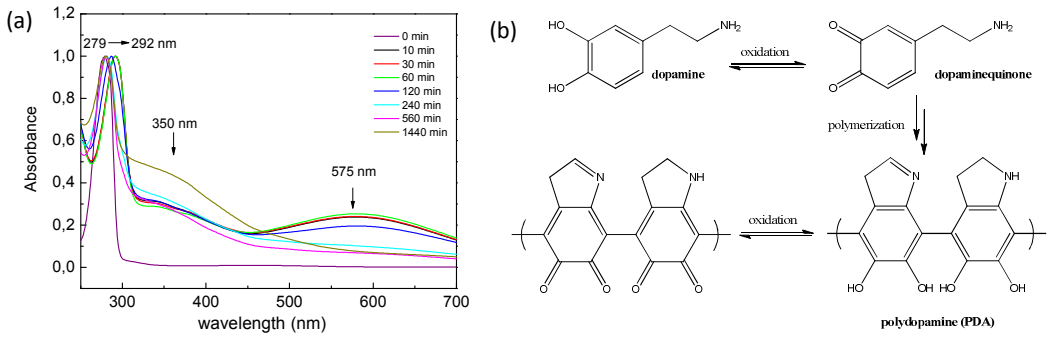

Figure 2. a) UV-vis absorption spectra of the supernatant at different mixing times and the reaction pathways for the formation of polydopamine. b) Proposed mechanism of the dopamine polymerization.

After 10 min running time when mixed the magnetite NPs with dopamine it is clearly observed an absorption band at 350 nm due to the formation of quinone which is in agreement with the proposed mechanism of polymerization (Figure 2b). Besides, an additional peak is appreciated at 575 nm concomitantly with a shift in the main absorption band from 279 to 292 nm that can be ascribed to the formation of catechol-Fe^{3+} complexes[2829]. Interestingly, the intensity of the broad band at 575 nm decreases with reaction time, disappearing completely after 24 h. Simultaneously, the absorption band at 292 nm shifts back gradually to 279 nm. This indicates that the catechol-Fe^{3+} complex formed at the beginning of the reaction vanishes from the supernatant

throughout the polymerization and deposition on the surface of the magnetic nanoparticles. After 24 h a typical spectrum of polydopamine is obtained in the supernatant.

Once it was shown that the polymerization takes place in the solution under relatively oxidative conditions due to the present of Fe^{3+}, the magnetite nanoparticles obtained after 24 h of mixing (Fe_3O_4@PDA-**1** NPs) were characterized in order to determine the formation of the polydopamine coating on the surface and compared with the naked particles prepared without the addition of dopamine. Since the magnetite core was first synthesized under the same experimental conditions as the naked NPs before the formation of the polymeric shell, it is expected similar diffractograms. In effect, both diffractograms show similar patterns (Figure 3), where all peaks can be indexed according to the Fd3m (227) spinel structure. Rietveld analysis results show a lattice parameter of 8.392 Å for the naked NPs and 8.385 Å for Fe_3O_4@PDA-**1** NPs and average crystallite size of 25(1) nm and 18(1), respectively. These structures were refined yielding low agreement factors, R_{Bragg} 5.840, R_f = 3.795 and R_{Bragg} 6.328, R_f = 3.730, respectively. The average crystalline sizes calculated from the broadening of the peak (311) by using Scherrer's equation were found to be 24 and 22 nm, for the naked and the coated NPs, respectively, in agreement with that calculated by using Rietveld method. It is demonstrated that the addition of dopamine does not affect the structure and size of magnetic nanoparticles because the nucleation and growth of the crystals occurred in the absence of dopamine. The most important parameter of nucleation and growing is the temperature,[30] in this approach it has been maintained constant at 25ºC. Nucleation involves the addition of atoms or molecules to a nucleus having the structure of the solid. If the nucleus is larger than a certain critical size, it will grow spontaneously, but if it is smaller than the critical size, the nucleus will be unstable.

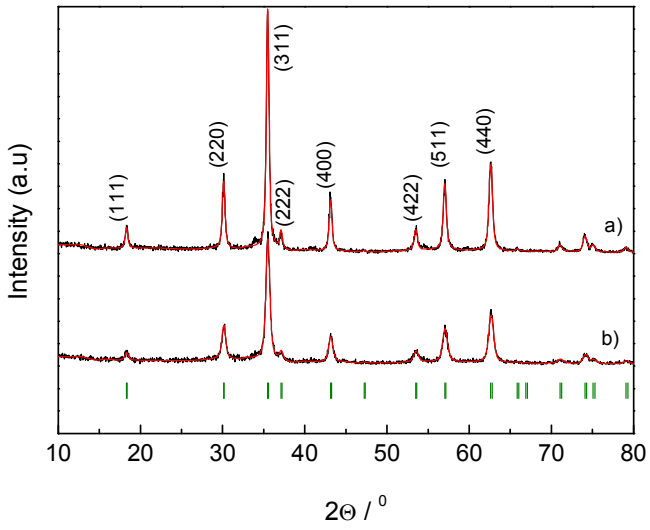

Figure 3. XRD patterns of a) naked magnetite nanoparticles synthesized electrochemically and b) magnetite nanoparticles coated with polydopamine synthesized by mixing the NPs with dopamine during 24 h (Fe_3O_4@PDA-**1** NPs). The black dots represent the observed data and the red lines show the calculated pattern obtained using the Rietveld analysis. Bragg positions are marked (|).

Regarding the dispersability in aqueous solution, visually the nanoparticles do not exhibit a good colloidal stability and lead to sedimentation in relatively short time, thus poor polydopamine coating is expected. Figure 4 shows the TEM images of the naked magnetite nanoparticles prepared via electrochemical route in a NaCl solution as well as the nanoparticles obtained after the addition of dopamine followed by 24 h of stirring at room temperature. In both cases the NPs are quasi-spherical with a mean diameter of 23 ± 4 nm and 20 ± 4 nm in good agreement with those estimated by XRD.

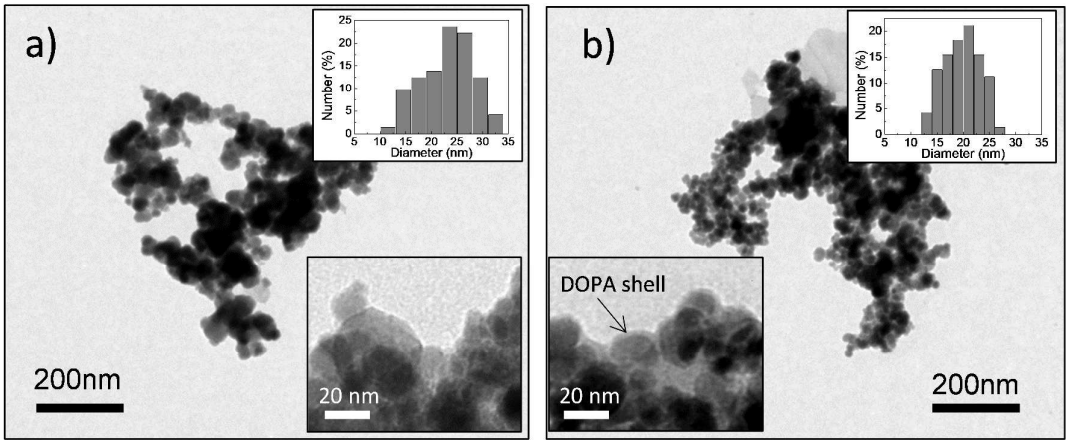

Figure 4. TEM images and particle size distributions of a) magnetite nanoparticles synthesized electrochemically and b) magnetite nanoparticles coated with polydopamine Fe_3O_4@PDA-**1** NPs.

It is clearly observed in Figure 4b that the magnetic nanoparticles obtained after the addition of dopamine present a polymeric shell with an average thickness of ca. 2.4 ± 0.3 nm (taking into account the shell thickness in different areas of the picture). Besides, the nanoparticles seem to be a bit more disperse in comparison with the naked magnetic nanoparticles (Figure 4a). The surface functionalization of the magnetite NPs was also confirmed by FTIR, TGA and Zeta potential measurements. Additional absorption bands at 1290 and 1486 cm^{-1} appear in the FTIR spectrum which are ascribed to the ν (C=C) and ν (C-N) of the polydopamine coating, respectively (Figure 5).[31]

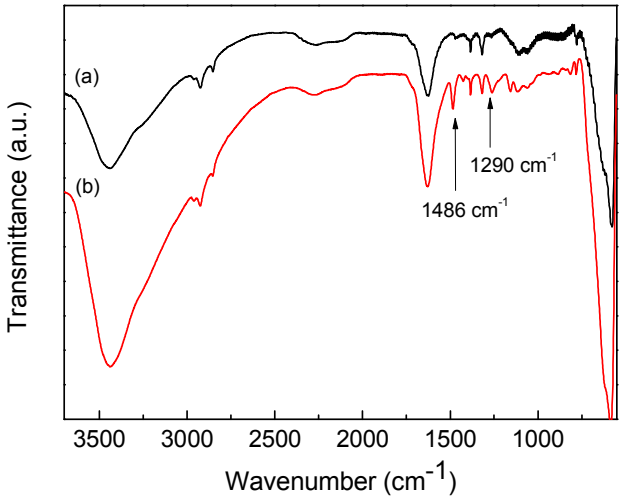

Figure 5. FTIR spectra of a) naked NPs synthesized electrochemically and b) of Fe_3O_4@PDA-**1** NPs.

However, the TGA and the Zeta potential analyses indicate a poor functionalization. The amount of polydopamine covering the nanoparticles quantified by TGA was estimated to be less than 2 wt. % (Figure S1 of Supporting Information). Similarly, Zeta potential experiments pointed out the low surface modification obtained by this strategy. Although a displacement of the value from -18 mV for naked NPs to -3 mV in case of Fe_3O_4@PDA-**1** NPs was achieved, negative Zeta potential value indicates an insufficient surface modification.

In order to favor the self-polymerization of dopamine and the formation of a polymeric shell around the nanoparticles, the dopamine was incorporated to the mixture at the beginning of the electrosynthesis of the magnetite NPs following the approach **2** (Scheme 1). In this condition the pH of the solution turns alkaline, pH~11, as a result of the reduction of water leading OH^-, and therefore the polymerization of dopamine can be induced by both alkaline pH and highly oxidative conditions. Since the magnetite is simultaneously formed during the process, the size of the magnetic core as well as the polymeric shell may be strongly affected by the amount of dopamine. Therefore, the

one step synthesis of core–shell magnetite nanoparticles via simultaneous oxidation of dopamine and iron was conducted varying the amount of dopamine added to the electrolyte solution, in particular 0.02, 0.05, 0.1 and 0.2 mg/mL. After 30 min the resulting magnetic materials were obtained (Fe_3O_4@PDA-**2**-0.02mg, Fe_3O_4@PDA-**2**-0.05mg, Fe_3O_4@PDA-**2**-0.1mg, Fe_3O_4@PDA-**2**-0.2mg NPs, respectively). It has to be mentioned that with the addition of 0.2 mg/mL of dopamine, the obtained product cannot be magnetically isolated possibly due to the poisoning of the electrode by the PDA and/or the formation of very small nanoparticles. The supernatants of the rest of the electrosyntheses (0.02, 0.05 and 0.1 mg/mL of dopamine) were then analyzed by UV-vis spectroscopy and the typical spectrum of PDA was appreciated with very low absorption intensity as a consequence of low concentration of polymer in the solution (data not shown). This seems to indicate that the self-polymerization of dopamine takes place preferentially on the surface of the NPs rather than in solution. Afterward the obtained magnetic nanoparticles were analyzed by XRD as displayed in Figure 6. As expected the diffractograms confirm the structure of spinel magnetite (Fd3m) with the following unit cell parameters and agreement factors calculated by Rietveld refinement: a=8.371 Å, R_{bragg}=5.795, R_f=3.311 for Fe_3O_4@PDA-**2**-0.02mg NPs; a=8.361 Å, R_{bragg}=5.633, R_f=3.685 for Fe_3O_4@PDA-**2**-0.05mg NPs. It is observed that the addition of dopamine at the beginning of the electrosynthesis significantly modified the crystal size of the magnetic NPs, decreasing the average size with the amount of dopamine incorporated to the solution, 14.5(6) nm (17 nm calculated by Scherrer) and 11.7(4) nm (8 nm calculated by Scherrer) for the addition of 0.02 and 0.05 mg/mL of dopamine, respectively. With the incorporation of 0.1 mg/mL the obtained nanoparticles were rather small and cannot be accurately measured, but comparing with the literature the size should be less than 5 nm[32]. These results are expected since the self-polymerization

of dopamine can occur on the surface of the iron oxide NPs that are formed during the process, impeding by this way the growing of the NPs. In addition, the polydopamine chains formed in the solution can also be adhered to the surface of the NPs. Contrary to the previous strategy (Approach **1**) the polymerization of dopamine takes place during the nucleation and growth of the particles and consequently the polydopamine adheres to the surface of the growing NPs strongly affecting the size of the final NPs.

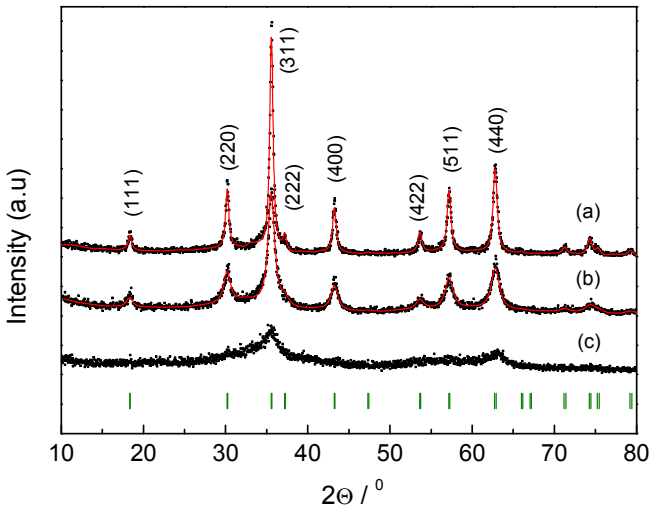

Figure 6. XRD patterns of magnetite nanoparticles synthesized electrochemically by approach **2**: a) Fe_3O_4@PDA-**2**-0.02mg, b) Fe_3O_4@PDA-**2**-0.05mg and c) Fe_3O_4@PDA-**2**-0.1mg. The black dots show the observed data and the red lines show the calculated pattern obtained using the Rietveld analysis. Bragg positions are marked (|).

To further investigate the development of polydopamine coating on the surface of the magnetite nanoparticles, the morphology of the magnetic materials was characterized by TEM. Figure 7a) shows that the resulting Fe_3O_4@PDA-**2**-0.02mg NPs forms aggregates with a clearly visible polymeric shell of 2.4 ± 0.4 nm around the clusters of nanoparticles.

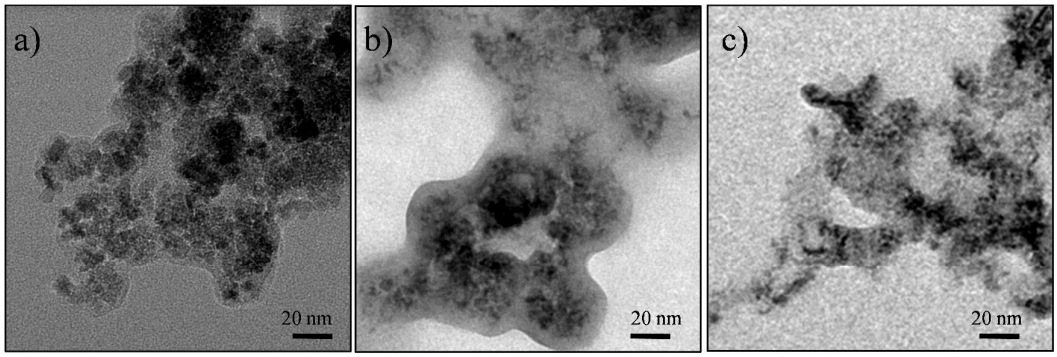

Figure 7. TEM images of magnetite nanoparticles synthesized electrochemically by approach **2**: a) Fe_3O_4@PDA-**2**-0.02mg, b) Fe_3O_4@PDA-**2**-0.05mg and c) Fe_3O_4@PDA-**2**-0.1mg.

Indeed, increasing the percentage of dopamine in the reaction medium leads to a dramatic diminishment of the NPs size, in agreement with XRD measurements, as well as the formation of large polymeric coating, appearing as a surrounding gray cover as depicted in Figure 7b and 7c. The huge coverage is very heterogeneous and involves groups of magnetite nanoparticles, making difficult the accurate measurement of the particle size by TEM. FTIR also confirms the present of polydopamine covering the NPs with two new bands at 1486 and 1290 cm^{-1} (Figure S2 of Supporting Information).

Furthermore, Zeta potential measurements demonstrate the increase in the polymeric coating with the amount of dopamine added to the mixture. All the synthetized NPs are positively charged as a consequence of the polydopamine coating and the Zeta potential augments from +7 to +29 mV for the sample Fe_3O_4@PDA-**2**-0.02mg and Fe_3O_4@PDA-**2**-0.1mg, respectively, corroborating the coverage increase. Table 1 summarizes the Zeta potential as well as the TGA results obtained for all the NPs.

Table 1. Zeta potential values, weight percentages of polydopamine and particle sizes (D) obtained for the polydopamine coated magnetite nanoparticles.

Sample	Zeta (mV)	wt. % polymer	D^{DRX} (nm)[a]	D^{TEM} (nm)
Fe_3O_4@PDA-**1**	-3	2	18(1)	21 ± 5
Fe_3O_4@PDA-**2**-0.02mg	+7	2	14.5(6)	[b]
Fe_3O_4@PDA-**2**-0.05mg	+29	11	11.7(4)	[b]
Fe_3O_4@PDA-**2**-0.1mg	+29	20	[b]	[b]
Fe_3O_4@PDA-**3**-0.2mg	+20	3	18(1)	15±4
Fe_3O_4@PDA-**3**-0.4mg	+22	3	17.6(4)	16±3
Fe_3O_4@PDA-**3**-0.6mg	+21	3	16.4(8)	17±4

[a] calculated by Rietveld analysis. [b] not accurate estimation

Thermogravimetric analysis under air atmosphere was carried out to quantify the polymeric coating created around the magnetic nanoparticles. As can be clearly seen in Table 1 and Figure S3 (see Supporting Information) the content of polydopamine increases with the amount of dopamine incorporated into the reaction up to ~20 wt. %. Clearly it has been demonstrated that the one step synthesis of PDA coated magnetic nanoparticles can be successfully carried out in a simple manner. The dopamine self-polymerizes simultaneously during the electrosynthesis of magnetite leading to nanoparticles with a large polymeric coverage. The size of the NPs and the percentage of PDA can be tuned in some extend by varying the content of dopamine added to the reaction mixture. In addition, the experiments were easily repeated and showed good reproducibility. However, the size of the magnetic nanoparticles dramatically decreases, fact that can affect the magnetic properties of the materials.

In order to study the nanoparticle size influence in the magnetic properties, magnetic measurements had been carried out. Magnetic hysteresis loops at 100 K, depicted in

Figure 8, show a near magnetic saturation for all samples. It is worth noting that despite the nanoparticle size decreases from 25 nm, in sample without polymer, to 11.7 nm, in Fe_3O_4@PDA-**2**-0.05mg, the magnetic saturation moment is almost the same. The M_S values were obtained after fitting the high magnetic field region to $M(H)=M_S+\chi_d H$, where M_S is the zero field saturation magnetization and χ_d the high field differential susceptibility. The results obtained, 78.5(1), 81.2(1) and 75.0(1) emu/g for naked, Fe_3O_4@PDA-**2**-0.02mg and Fe_3O_4@PDA-**2**-0.05mg samples, respectively, show a independence particle-size magnetic saturation with values near to the bulk material (92 emu/g)[33] and very similar to previously reported values for magnetite NPs.[34] On the other hand, Fe_3O_4@PDA-**2**-0.1mg shows a magnetic moment four time lower, 14.3(1) emu/g, that could be due to the spin disorder in the surface and in agreement with reported values for nanoparticles with similar sizes.[32] The inset of Figure 8 shows a zoom of hysteresis loops. As it can be observed, the coercivity field decreases with the polymeric coverage from 175, 78, 9 and 4 Oe for naked NPs, Fe_3O_4@PDA-**2**-0.02mg, Fe_3O_4@PDA-**2**-0.05mg and Fe_3O_4@PDA-**2**-0.1mg, respectively. This progress points out the magnetic evolution from a superferromagnetic to a superparamagnetic behavior.[32] The zero-field-cooling (ZFC) and field-cooling (FC) curves of Fe_3O_4@PDA-**2**-0.05mg and Fe_3O_4@PDA-**2**-0.1mg at 100 Oe, displayed in Figure 9, present a characteristic nanoparticle behavior. Fe_3O_4@PDA-**2**-0.1mg shows a blocking temperature around 91 K confirming the superparamagnetic behavior above this temperature.[35] Whereas Fe_3O_4@PDA-**2**-0.05mg ZFC-FC curves shows a large dipolar interaction between nanoparticles, exhibiting a badly defined blocking temperature.

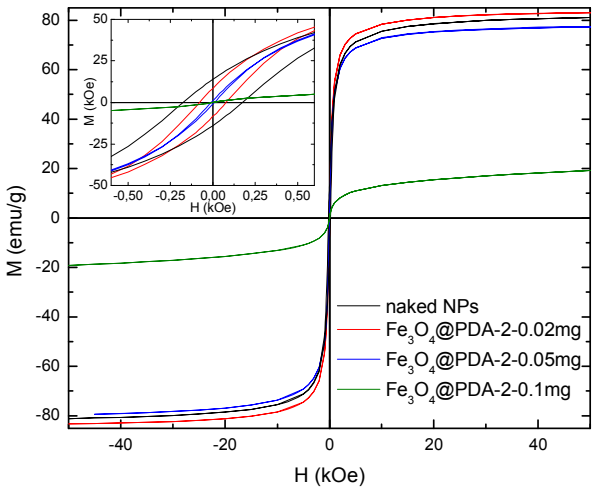

Figure 8. Hysteresis loops at 100 K, M(H), measured for naked NPs (black line), Fe_3O_4@PDA-**2**-0.02mg (red line), Fe_3O_4@PDA-**2**-0.05mg (blue line) and Fe_3O_4@PDA-**2**-0.1mg (green line). The inset shows a zoom of the low magnetic field.

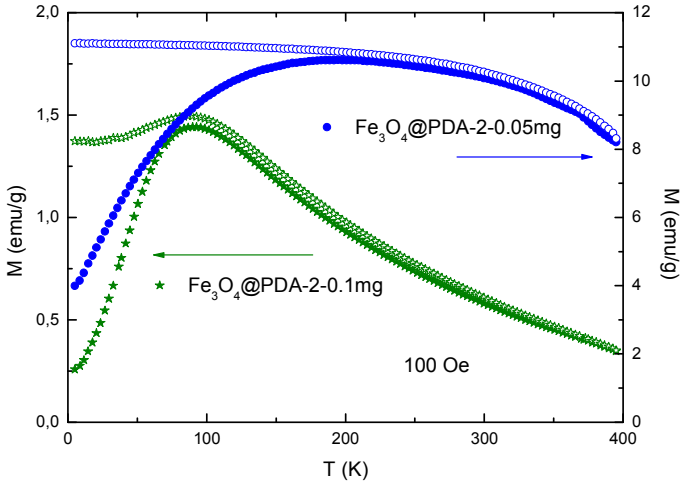

Figure 9. ZFC/FC curves for Fe_3O_4@PDA-**2**-0.05mg (blue line) and Fe_3O_4@PDA-**2**-0.1mg (green line) measured with H = 100 Oe.

Subsequently another approach was explored to obtain water dispersible magnetic nanoparticles with a more homogeneous polydopamine shell and preserving the size of the magnetic core, approach **3**. Specifically the electrosynthesis of magnetite nanoparticles was first started and after 20 min the dopamine was incorporated to the

solution maintaining the current during 10 min, that is, 30 min of total time. In a first attempt 0.2 mg/mL of dopamine, as in the previous approaches, was added to the mixture. XRD measurement (see Figure 10) shows all the peaks assigned with the spinel structure and a crystal size of 18 nm (calculated by both Rietveld's and Scherrer's methods), smaller than that obtained for the naked particles, 25 nm. Therefore, the incorporation of the dopamine once the process of the magnetite synthesis has been already started, leads to a reduction of the particle size but less dramatic as compared with its addition at the beginning of the synthesis. Then, we can assume that the magnetite nanocrystals are mainly formed during the first 20 min of the electrosynthesis. The subsequent addition of dopamine only affects slightly the growing process, lowering the crystal size but in less extend compared with the Approach **2**.

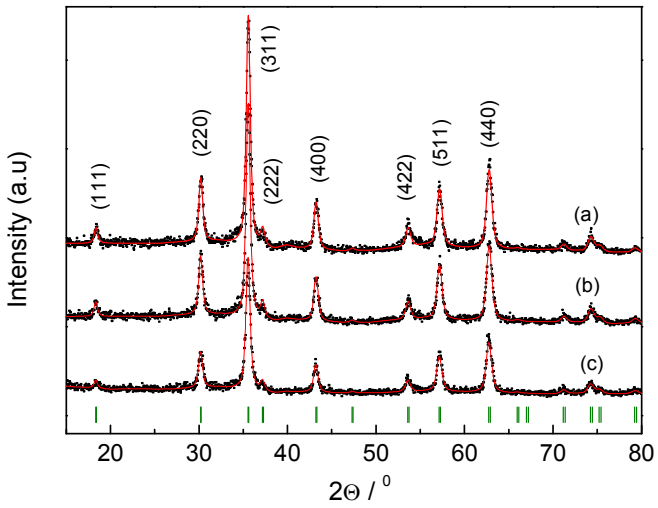

Figure 10. XRD patterns of magnetite NPs synthesized electrochemically by approach **3**: a) Fe_3O_4@PDA-**3**-0.2mg (a=8.373 Å, R_{Bragg}=7.396, R_f=4.307), b) Fe_3O_4@PDA-**3**-0.4mg (a=8.370 Å, R_{Bragg}=6.846, R_f=3.821) and c) Fe_3O_4@PDA-**3**-0.6mg (a=8.373 Å, R_{Bragg}=9.266, R_f=6.071). The black dots show the observed data and the red lines show the calculated pattern obtained using the Rietveld analysis. Bragg positions are marked (|).

The particles size determined from the TEM measurements is ~15 ± 4 nm which is in agreement with the size obtained from XRD. Additionally, the TEM micrographs shows a relatively good homogeneity and low aggregation of nanoparticles in which a polymeric layer with a thickness of ca. 3.3 ± 0.5 nm is easily distinguished around them (Figure 11a).

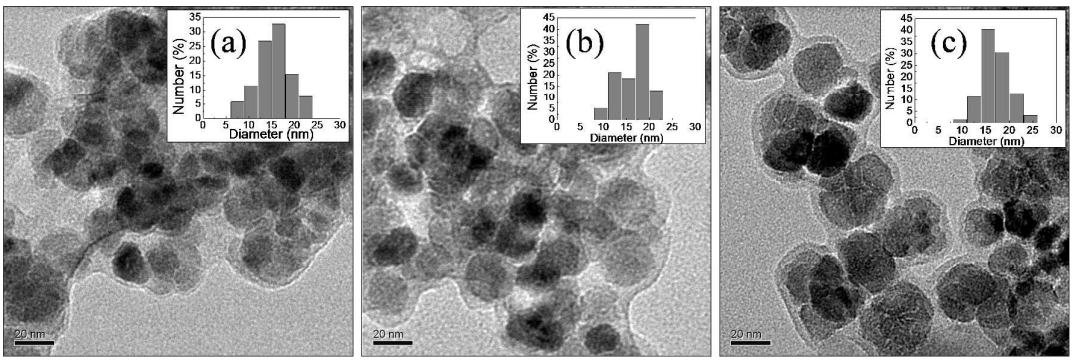

Figure 11. TEM images and particle size distribution of magnetite NPs synthesized electrochemically by approach **3**: a) Fe_3O_4@PDA-**3**-0.2mg, b) Fe_3O_4@PDA-**3**-0.4mg and c) Fe_3O_4@PDA-**3**-0.6mg.

FTIR experiments also confirm the presence of PDA in the magnetic materials with the appearance of bands corresponding to the polymer (Figure S4 of Supporting Information). Although the percentage of PDA that covers the NPs estimated by TGA did not exceed the 3 wt. % (see Figure S5 of Supporting Information), Zeta potential measurements demonstrated a relatively good colloidal stability in aqueous solution with value of ca. +20 mV (Table 1). With the purpose of increasing the thickness of the polydopamine layer without altering the size of the magnetic core, higher amounts of dopamine, 0.4 and 0.6 mg/mL, were incorporated to the electrosynthesis medium after 20 min of reaction following the approach **3**. The XRD and TGA measurements of the resulting magnetic nanoparticles demonstrated that increasing the content of dopamine produces neither an obvious decrease of the magnetic core nor a significantly increase

in the thickness layer, as can be seen in Table 1 and Figures 10. Only a slightly increases in the thickness layer is appreciable in the TEM image, 5.3 ± 0.5 nm and 5.0 ± 0.8 nm for the Fe_3O_4@PDA-**3**-0.4mg and Fe_3O_4@PDA-**3**-0.6mg NPs, respectively.

Figure 12 shows the magnetic hysteresis loops of naked and Fe_3O_4@PDA-**3**-0.4mg NPs. The shape of both is similar but the magnetic saturation moments changes noteworthy, from 78.5(1) to 60.2(1) emu/g. This decrease is normally associated to the nanoparticle decrease, in this case from 25 nm for naked to ~18 nm for polymer coated nanoparticles, see Table 1. The decrease of nanoparticle size entails an increase of surface-volume ratio and surface effects are enhanced, where the spins are usually misaligned. However, it is reported in previous work[36] that there is an electron transfer from the dopamine to the octahedral Fe sites located at the surface of the NP that could lead to significant changes in the magnetic properties. For instance, this can introduce some kind of disorder in the surface, inhibiting the spin orientation and reducing the magnetic saturation moment. In the same way, the coercivity field decreases from 179 Oe for naked NPs to 115 Oe for Fe_3O_4@PDA-**3**-0.4mg (see inset of Figure 12).

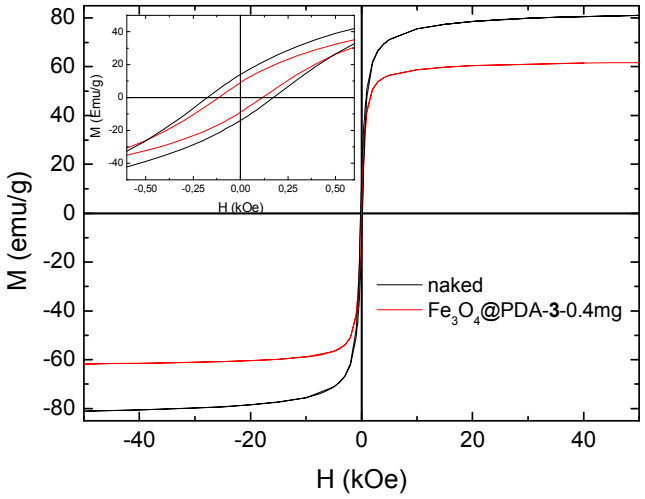

Figure 12. Hysteresis loops, M(H), measured for naked NPs (black line) and Fe_3O_4@PDA-**3**-0.4mg (red line). The inset shows a zoom of the low magnetic field.

These changes in magnetic properties as a consequence of the polydopamine coating is more notable in samples synthesized by approach **3** because the polydopamine tends to cover individual NPs rather than groups of NPs as in the approach **2**.

Conclusions

In summary, we have presented the one step synthesis of magnetite nanoparticles coated with polydopamine via electrochemical route. This strategy allows the preparation of magnetite nanoparticles in a very simple and rapid manner. The reaction conditions, alkaline pH and oxidative environment, also favor the self-polymerization of dopamine simultaneously with the magnetite formation. It has been demonstrated the versatility of this strategy, in which different approaches can be carried out tuning the size of both the core and the polymeric shell. On one hand, approach **1**, in which the polymerization of dopamine only involves oxidative conditions by Fe^{3+} ions, conducts to a thin polymeric coverage. Besides, the incorporation of dopamine does not modify the magnetic core, as it was added at the end of the electrosynthesis. Second approach leads to a significant decrease in the NPs size concomitantly with the formation of the PDA layer coating clusters of NPs. As the polymerization of dopamine takes place at the same time as the nucleation and growth of the magnetite nanocrystals, the final size of the core is strongly affected. Finally, in the third approach the dopamine polymerization starts once the magnetic nanoparticles are almost formed. As a result the size of the core does not diminish significantly and this strategy allows the coverage of individual NPs. The variety of obtained magnetic materials from individual nanoparticles to cluster of

nanoparticles, together with the outstanding properties of polydopamine make this method very attractive for a wide range of applications.

Acknowledgements

This work was financially supported by the Spanish MINECO (Project MAT2012-37109-C02-02). A. Muñoz-Bonilla gratefully acknowledges the MINECO for her Ramon y Cajal contract.

References

1. S. Shylesh, V. Schünemann, and W. R. Thiel, *Angew. Chem. Int. Ed. Engl.*, 2010, **49**, 3428–59.

2. B. D. Terris and T. Thomson, *J. Phys. D. Appl. Phys.*, 2005, **38**, R199–R222.

3. S. C. N. Tang and I. M. C. Lo, *Water Res.*, 2013, **47**, 2613–32.

4. F. Xu, J. H. Geiger, G. L. Baker, and M. L. Bruening, *Langmuir*, 2011, **27**, 3106–12.

5. S. Laurent, D. Forge, M. Port, A. Roch, C. Robic, L. Vander Elst, and R. N. Muller, *Chem. Rev.*, 2008, **108**, 2064–110.

6. M. Colombo, S. Carregal-Romero, M. F. Casula, L. Gutiérrez, M. P. Morales, I. B. Böhm, J. T. Heverhagen, D. Prosperi, and W. J. Parak, *Chem. Soc. Rev.*, 2012, **41**, 4306–34.

7. M. Guo, C. Que, C. Wang, X. Liu, H. Yan, and K. Liu, *Biomaterials*, 2011, **32**, 185–94.

8. K. Turcheniuk, A. V Tarasevych, V. P. Kukhar, R. Boukherroub, and S. Szunerits, *Nanoscale*, 2013, **5**, 10729–52.

9. R. C. Sealy, J. S. Hyde, C. C. Felix, I. a Menon, and G. Prota, *Science*, 1982, **217**, 545–7.

10. J. Riesz, J. Gilmore, and P. Meredith, *Biophys. J.*, 2006, **90**, 4137–44.

11. S. H. Ku, J. Ryu, S. K. Hong, H. Lee, and C. B. Park, *Biomaterials*, 2010, **31**, 2535–41.

12. A. B. Mostert, B. J. Powell, F. L. Pratt, G. R. Hanson, T. Sarna, I. R. Gentle, and P. Meredith, *Proc. Natl. Acad. Sci. U. S. A.*, 2012, **109**, 8943–7.

13. H. Lee, S. M. Dellatore, W. M. Miller, and P. B. Messersmith, *Science*, 2007, **318**, 426–30.

14. Q. Wei, F. Zhang, J. Li, B. Li, and C. Zhao, *Polym. Chem.*, 2010, **1**, 1430.

15. Y. Liu, K. Ai, and L. Lu, *Chem. Rev.*, 2014, **114**, 5057–115.

16. R. Liu, S. M. Mahurin, C. Li, R. R. Unocic, J. C. Idrobo, H. Gao, S. J. Pennycook, and S. Dai, *Angew. Chem. Int. Ed. Engl.*, 2011, **50**, 6799–802.

17. H. Jiang, T. Sun, C. Li, and J. Ma, *RSC Adv.*, 2011, **1**, 954.

18. J. Cui, Y. Yan, G. K. Such, K. Liang, C. J. Ochs, A. Postma, and F. Caruso, *Biomacromolecules*, 2012, **13**, 2225–8.

19. M. d'Ischia, A. Napolitano, A. Pezzella, P. Meredith, and T. Sarna, *Angew. Chem. Int. Ed. Engl.*, 2009, **48**, 3914–21.

20. K. C. L. Black, Z. Liu, and P. B. Messersmith, *Chem. Mater.*, 2011, **23**, 1130–1135.

21. R. Liu, Y. Guo, G. Odusote, F. Qu, and R. D. Priestley, *ACS Appl. Mater. Interfaces*, 2013, **5**, 9167–71.

22. R. Mrówczyński, R. Turcu, C. Leostean, H. a. Scheidt, and J. Liebscher, *Mater. Chem. Phys.*, 2013, **138**, 295–302.

23. E. Zhang, M. Kircher, and M. Koch, *ACS nano ...*, 2014, 3192–3201.

24. R. Mrówczyński, A. Bunge, and J. Liebscher, *Chem. - A Eur. J.*, 2014, **20**, 8647–53.

25. L. Cabrera, S. Gutierrez, N. Menendez, M. P. Morales, and P. Herrasti, *Electrochim. Acta*, 2008, **53**, 3436–3441.

26. J. Rodríguez-Carvajal, *Phys. B Phys. Condens. Matter*, 1993, **192**, 55–69.

27. L. Yang, J. Kong, D. Zhou, J. M. Ang, S. L. Phua, W. A. Yee, H. Liu, Y. Huang, and X. Lu, *Chem. - A Eur. J.*, 2014, **20**, 7776–83.

28. G. H. Hwang, K. H. Min, H. J. Lee, H. Y. Nam, G. H. Choi, B. J. Kim, S. Y. Jeong, and S. C. Lee, *Chem. Commun. (Camb).*, 2014, **50**, 4351–3.

29. M. J. Sever and J. J. Wilker, *Dalt. Trans.*, 2004, 1061–1072.

30. E. Mazario, M. P. Morales, R. Galindo, P. Herrasti, and N. Menendez, *J. Alloys Compd.*, 2012, **536**, S222–S225.

31. Y. Ma, X. Zhang, T. Zeng, D. Cao, Z. Zhou, W. Li, H. Niu, and Y. Cai, *ACS Appl. Mater. Interfaces*, 2013, **5**, 1024–30.

32. G. F. Goya, T. S. Berquó, F. C. Fonseca, and M. P. Morales, *J. Appl. Phys.*, 2003, **94**, 3520.

33. B. D. Cullity, *Introduction to Magnetic Materials*, Reading, Addison-We., 1972.

34. P. Guardia, B. Batlle-Brugal, a. G. Roca, O. Iglesias, M. P. Morales, C. J. Serna, a. Labarta, and X. Batlle, *J. Magn. Magn. Mater.*, 2007, **316**, e756–e759.

35. J. Alonso, M. L. Fdez-Gubieda, J. M. Barandiarán, a. Svalov, L. Fernández Barquín, D. Alba Venero, and I. Orue, *Phys. Rev. B*, 2010, **82**, 054406.

36. J. Fouineau, K. Brymora, L. Ourry, F. Mammeri, N. Yaacoub, F. Calvayrac, and J. Greneche, *J. Phys. Chem. C*, 2013, **117**, 14295–14302.